Electronic Supplementary Material (ESI) for Dalton Transactions.

Three novel metal-organic frameworks with different coordination modes for trace detection of anthrax biomarkers

Zhenzhong Cong,[a] Mingchang Zhu,[b] Ying Zhang,[b] Wei Yao,[a] Marina Kosinova,[c] Vladimir P. Fedin,[c] Shuangyan Wu[b] and Enjun Gao*[a,b]*

Table S1 Crystallographic data of **MOF 1**

parameter	$\{[Ca_3(ddpa)\cdot 7H_2O]\}_n$
Formula	$C_{24}H_{22}Ca_3O_{22}$
Formula weight	782.65 g/mol
Crystal system	*Monoclinic*
Space group	$P2_1/c$
a / Å	7.9374(2)
b / Å	22.5281(5)
c / Å	19.6837(5)
α / °	90
β / °	92.9800(10)
γ / °	90
V (Å^3)	3514.97(15)
Z	4
ρ_{calc}g/cm^3	1.479
The Range for data Collection	4.144 to 52.742
Data / restraints / parameters	2736 / 7 / 210
Independent reflections	7169[R_{int}=0.0493,R_{sigma}=0.0282]
Completeness / %	99.9%
GOF on F^2	1.082
Final R indices(I > 2σ(I))	R_1=0.0548,wR_2=0.1643
R indices (all data)	R_1=0.0662,wR_2=0.1751
Largest diff. peak / hole / eÅ^{-3}	1.91 / -0.70

$^aR_1 = \sum||F_0| - |F_c||/\sum|F_0|$. $^bwR_2 = [\sum w(F_0^2 - F_c^2)^2/\sum w(F_0^2)^2]^{1/2}$

Table S2 Selected bond lengths (Å) and angles (°) for the **MOF 1**

Bond	Length/Å	Bond	Length/Å
Ca1-O11[1]	2.416(2)	Ca1-O8[3]	2.441(2)
Ca1-O13	2.484(2)	Ca1-O2[4]	2.382(4)
Ca1-O7[3]	2.403(2)	Ca1-O3[5]	2.457(2)
Ca1-O15	2.562(2)	Ca1 O14	2.664(2)
Ca2-O8[6]	2.504(2)	Ca2-O13[7]	2.353(2)
Ca2-O20	2.424(3)	Ca2-O21	2.328(2)
Ca2-O9[6]	2.462(2)	Ca2-O6	2.340(3)
Ca2-C14[6]	2.828(3)	Ca2-O22	2.417(7)
Ca3-O11[2]	2.725(2)	Ca3-O15	2.402(2)
Ca3-O14	2.447(2)	Ca3-O12[2]	2.468(3)
Ca3-O19	2.392(3)	Ca3-O18	2.370(3)
Ca3-O16	2.496(4)	Ca3-O17	2.443(5)
Angle	ω/°	Angle	ω/°
O7[3]-Ca1-O14	136.50(8)	O18-Ca3-O11[1]	76.77(10)
O11[1]-Ca1-O8[3]	74.76(8)	O18-Ca3-O15	138.13(11)
O11[1]-Ca1-O13	95.96(8)	O18-Ca3-O14	78.68(12)
O11[1]-Ca1-O3[4]	137.10(8)	O18-Ca3-O12[1]	84.50(12)
O11[1]-Ca1-O15	68.09(8)	O18-Ca3-O19	120.69(12)
O11[1]-Ca1-O14	73.73(7)	O18-Ca3-O16	135.18(17)
C10-C11-C13	118.8(3)	O18-Ca3-O17	73.33(15)
O8[3]-Ca1-O13	71.83(7)	O16-Ca3-O11[1]	111.98(11)
O8[3]-Ca1-O3[4]	140.50(8)	O17-Ca3-O11[1]	139.05(12)
O8[3]-Ca1-O15	142.31(8)	O17-Ca3-O14	126.77(14)
O8[3]-Ca1-O14	108.68(8)	O17-Ca3-O12[1]	99.42(13)
O3[4]-Ca1-O14	71.41(8)	O17-Ca3-O16	73.46(17)
O13-Ca1-O15	117.39(8)	O14-Ca3-O12[1]	122.01(8)
O13-Ca1-O14	50.52(7)	O21-Ca2-O8[6]	152.51(9)
O3[4]-Ca1-O13	80.57(8)	O21-Ca2-O13[7]	87.26(9)
O2[5]-Ca1-O11[1]	91.88(8)	O21-Ca2-O20	83.49(9)
O2[5]-Ca1-O8[3]	100.12(8)	O21-Ca2-O9[6]	152.15(9)
O2[5]-Ca1-O13	166.74(8)	O21-Ca2-O6	96.26(10)
O2[5]-Ca1-O7[3]	74.83(8)	O9[6]-Ca2-O8[6]	52.92(7)
O2[5]-Ca1-O3[4]	100.84(8)	O21-Ca2-O22	76.75(19)
O2[5]-Ca1-O15	75.50(8)	O15-Ca3-O14	73.08(8)
O2[5]-Ca1-O14	142.53(8)	O15-Ca3-O12[1]	84.96(9)
O3[4]-Ca1-O15	75.74(8)	O13[7]-Ca2-O8[6]	72.94(8)
O7[3]-Ca1-O11[1]	141.03(8)	O13[7]-Ca2-O20	84.41(8)
O7[3]-Ca1-O8[3]	71.94(8)	O13[7]-Ca2-O9[6]	98.97(9)

O7[3]-Ca1-O13	92.43(8)	O15-Ca3-O16	78.39(14)
O7[3]-Ca1-O3[4]	81.81(8)	O15-Ca3-O17	148.49(14)
O7[3]-Ca1-O15	138.30(8)	O13[7]-Ca2-O2[2]	85.3(2)
O20-Ca2-O8[6]	75.93(8)	O14-Ca3-O11[1]	72.17(7)
O13[7]-Ca2-O20	84.41(8)	O22-Ca2-O9[6]	76.76(18)

[1]+X,1/2-Y,-1/2+Z; [2]1-X,-1/2+Y,1/2-Z; [3]2-X,-1/2+Y,1/2-Z; [4]1+X,+Y,+Z; [5]1+X,1/2-Y,-1/2+Z; [6]-1+X,+Y,+Z; [7]1-X,1/2+Y,1/2-Z; [8]+X,1/2-Y,1/2+Z; [9]2-X,1/2+Y,1/2-Z; [10]-1+X,1/2-Y,1/2+Z

Table S3 Crystallographic data of **MOF 2**

parameter	$\{[Cd_3(ddpa)\cdot 6H_2O]\cdot 4H_2O\}_n$
Formula	$C_{24}H_{28}Cd_3O_{25}$
Formula weight	1053.66 g/mol
Crystal system	*Monoclinic*
Space group	C2/c
a / Å	18.184(2)
b / Å	13.6565(13)
c / Å	14.5002(15)
α / °	90
β / °	113.959(3)
γ / °	90
V (Å^3)	3290.6(6)
Z	4
ρ_{calc}g/cm^3	2.127
The Range for data Collection	5.52 to 50.064
Data / restraints / parameters	2888/0/238
Independent reflections	2888[R_{int}=0.0690,R_{sigma}=0.0571]
Completeness / %	99.9%
GOF on F^2	1.084
Final R indices(I > 2σ(I))	R_1=0.0388,wR_2=0.0902
R indices (all data)	R_1=0.0608,wR_2=0.1009
Largest diff. peak / hole / eÅ^{-3}	1.05/-0.60

[a]$R_1 = \sum||F_0| - |F_c||/\sum|F_0|$. [b]$wR_2 = [\sum w(F_0^2 - F_c^2)^2/\sum w(F_0^2)^2]^{1/2}$

Table S4 Selected bond lengths (Å) and angles (°) for the **MOF 2**

Bond	Length/Å	Bond	Length/Å
Cd1-O3[3]	2.281(4)	Cd2-O1[6]	2.328(4)

Cd1-O3	2.281(4)	Cd2-O2^{6}	2.409(4)
Cd1-O7^{4}	2.321(4)	Cd2-O4^{7}	2.225(4)
Cd1-O7^{5}	2.321(4)	Cd2-O6	2.208(4)
Cd1-O10^{3}	2.232(5)	Cd2-O8	2.323(5)
Cd1-O10	2.232(5)	Cd2-O9	2.419(4)
Angle	ω/°	Angle	ω/°
O4^{7}-Cd2-O8	90.86(18)	O10^{3}-Cd1-O3	88.93(16)
O4^{7}-Cd2-O9	82.38(15)	O10^{3}-Cd1-O3^{3}	91.07(16)
O4^{7}-Cd2-O2^{6}	146.71(15)	O10-Cd1-O3^{3}	88.93(16)
O6-Cd2-O1^{6}	141.74(15)	O10-Cd1-O3	91.07(16)
O6-Cd2-O2^{6}	92.34(16)	O10^{3}-Cd1-O7^{4}	88.20(16)
O6-Cd2-O4^{7}	116.92(16)	O10^{3}-Cd1-O7^{5}	91.80(17)
O6-Cd2-O8	117.00(17)	O10-Cd1-O7^{4}	91.79(16)
O6-Cd2-O9	81.98(15)	O10-Cd1-O7^{5}	88.21(16)
O4^{7}-Cd2-O1^{6}	91.83(15)	O10^{3}-Cd1-O10	180
O8-Cd2-O1^{6}	85.05(16)	O7^{5}-Cd1-O7^{4}	180
O8-Cd2-O2^{6}	89.24(18)	O1^{6}-Cd2-O2^{6}	55.02(14)
O8-Cd2-O9	160.76(16)	O1^{6}-Cd2-O9	77.22(15)
O3^{3}-Cd1-O3	180.00(12)	O3-Cd1-O7^{5}	90.09(14)
O3^{3}-Cd1-O7^{4}	90.08(14)	O2^{6}-Cd2-O9	86.71(16)
O3-Cd1-O7^{4}	89.91(14)	O3^{3}-Cd1-O7^{5}	89.92(14)

^{1}1/2+X,1/2-Y,1/2+Z; ^{2}1-X,+Y,1/2-Z; ^{3}1-X,2-Y,1-Z; ^{4}1-X,1-Y,1-Z; ^{5}+X,1+Y,+Z; ^{6}-1/2+X,1/2-Y,-1/2+Z; ^{7}+X,-1+Y,+Z

Table S5 Crystallographic data of **MOF 3**

parameter	$\{[Zn_3(ddpa)\cdot 2H_2O]\}_n$
Formula	$C_{24}H_{13}O_{17}Zn_3$
Formula weight	769.45 g/mol
Crystal system	*Monoclinic*
Space group	$P2_1/n$
a / Å	10.2364(5)
b / Å	13.3601(8)
c / Å	29.3596(18)
α / °	90
β / °	93.623(2)
γ / °	90
V (Å^3)	4007.2(4)
Z	4
ρ_{calc}g/cm^3	1.275

The Range for data Collection	4.304 to 52.042
Data / restraints / parameters	7900/19/385
Independent reflections	7900[R_{int}=0.0551,R_{sigma}=0.0298]
Completeness / %	99.9%
GOF on F^2	1.077
Final R indices(I > 2σ(I))	R_1=0.0578,wR_2=0.1743
R indices (all data)	R_1=0.0706,wR_2=0.1877
Largest diff. peak / hole / eÅ^{-3}	2.18/-1.14

$^{a}R_1 = \sum||F_0| - |F_c||/\sum|F_0|$. $^{b}wR_2 = [\sum w(F_0^2 - F_c^2)^2/\sum w(F_0^2)^2]^{1/2}$

Table S6 Selected bond lengths (Å) and angles (°) for the **MOF 3**

Bond	Length/Å	Bond	Length/Å
Zn1-O1^1	1.983(3)	Zn2-O11^5	1.976(3)
Zn1-O4	2.010(4)	Zn2-O17	1.945(3)
Zn1-O6^2	2.375(4)	Zn3-O3^6	2.105(5)
Zn1-O13^3	2.063(4)	Zn3-O9^3	2.107(5)
Zn1-O17^2	2.003(3)	Zn3-O14	2.038(6)
Zn2-O7	1.946(3)	Zn3-O15	2.087(6)
Zn2-O8^4	1.964(3)	Zn3-O16	2.075(6)
Zn3-O17^7	2.080(3)		
Angle	ω/°	Angle	ω/°
O1^1-Zn1-O4	104.18(16)	O15-Zn3-O9^3	86.5(3)
O1^1-Zn1-O6^2	84.68(15)	O16-Zn3-O3^6	88.8(2)
O1^1-Zn1-O13^3	97.53(15)	O16-Zn3-O9^3	86.2(2)
O1^1-Zn1-O17^2	134.90(15)	O16-Zn3-O15	89.9(2)
O4-Zn1-O6^2	86.45(15)	O16-Zn3-O17^7	179.28(19)
O4-Zn1-O13^3	96.09(16)	O17^7-Zn3-O3^6	90.64(16)
O13^3-Zn1-O6^2	176.10(15)	O17^7-Zn3-O9^3	94.19(16)
O17^2-Zn1-O4	118.83(14)	O17^7-Zn3-O15	90.69(18)
O17^2-Zn1-O6^2	85.04(14)	O15-Zn3-O3^6	172.0(2)
O17^2-Zn1-O13^3	91.14(15)	Zn1^2-O17-Zn3^9	105.50(14)
O7-Zn2-O8^4	105.80(15)	Zn2-O17-Zn1^2	119.08(16)
O7-Zn2-O11^5	106.57(15)	Zn2-O17-Zn3^9	114.66(15)
O8^4-Zn2-O11^5	100.65(16)	O14-Zn3-O3^6	95.0(2)
O17-Zn2-O7	119.66(14)	O14-Zn3-O9^3	176.5(2)
O17-Zn2-O8^4	115.09(14)	O14-Zn3-O15	92.9(2)
O17-Zn2-O11^5	107.12(14)	O14-Zn3-O16	90.4(2)
O3^6-Zn3-O9^3	85.5(2)	O14-Zn3-O17^7	89.26(18)

^{1}1+X,+Y,+Z; ^{2}2-X,1-Y,1-Z; ^{3}3/2-X,1/2+Y,3/2-Z; ^{4}2-X,-Y,1-Z; ^{5}1-X,-Y,1-Z; ^{6}3/2-X,-1/2+Y,3/2-Z; ^{7}-1/2+X,1/2-Y,1/2+Z

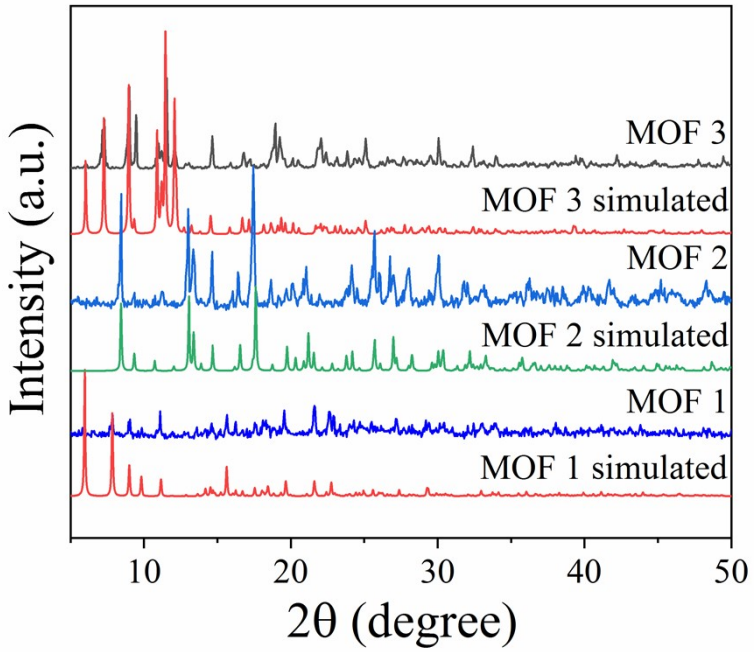

Figure S1 PXRD patterns of **MOFs 1-3**.

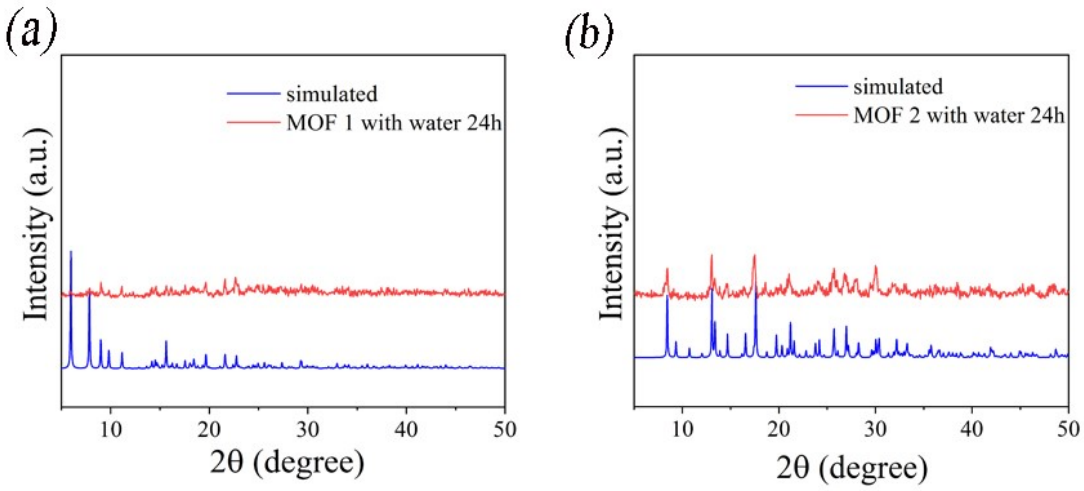

Figure S2 PXRD patterns of **MOFs 1** and **2** after immersion in water for 24h.

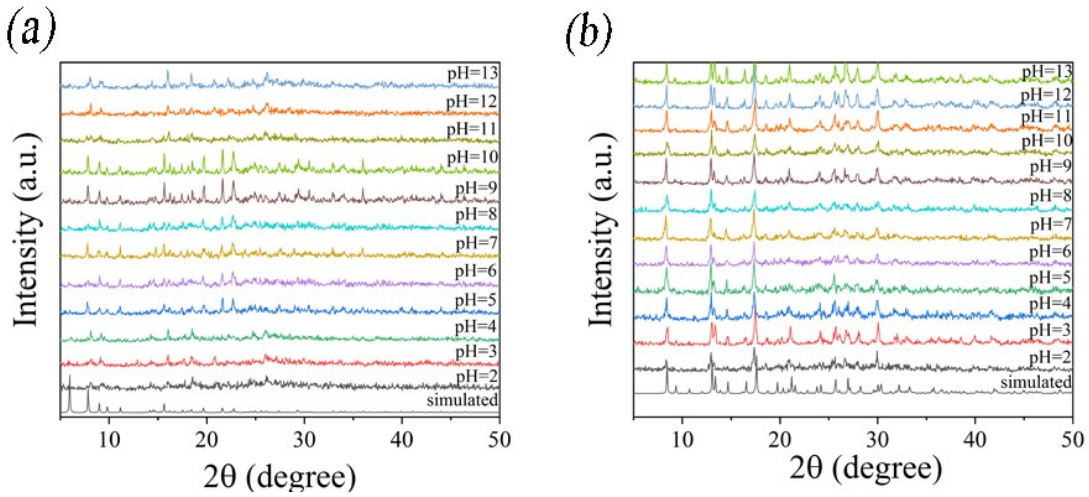

Figure S3 PXRD patterns of **MOFs 1** and **2** after treated by aqueous solutions with various pH values from 2 to 13.

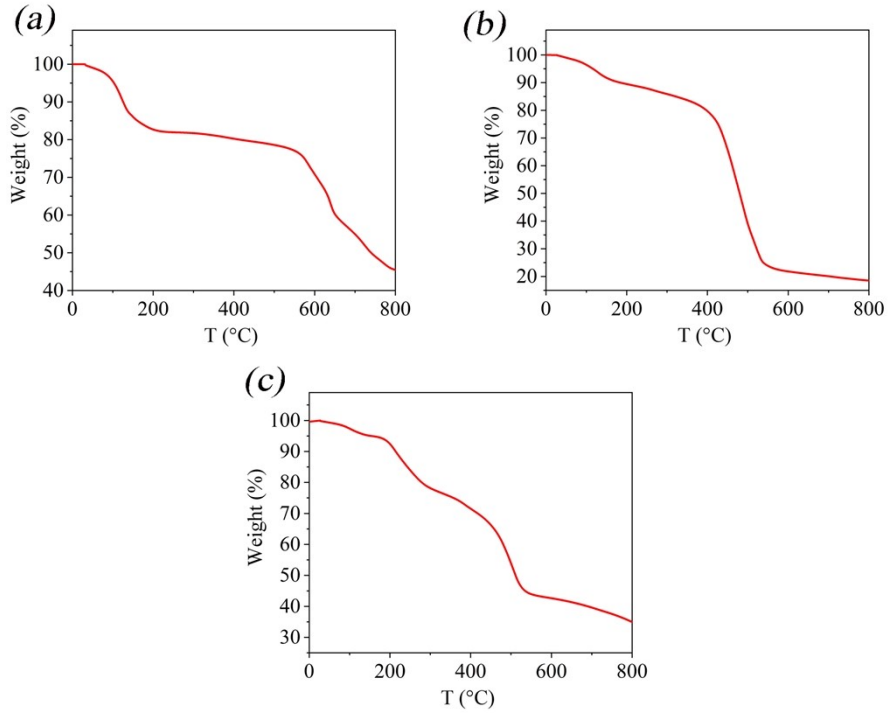

Figure S4 The TGA curves of **MOFs 1-3**.

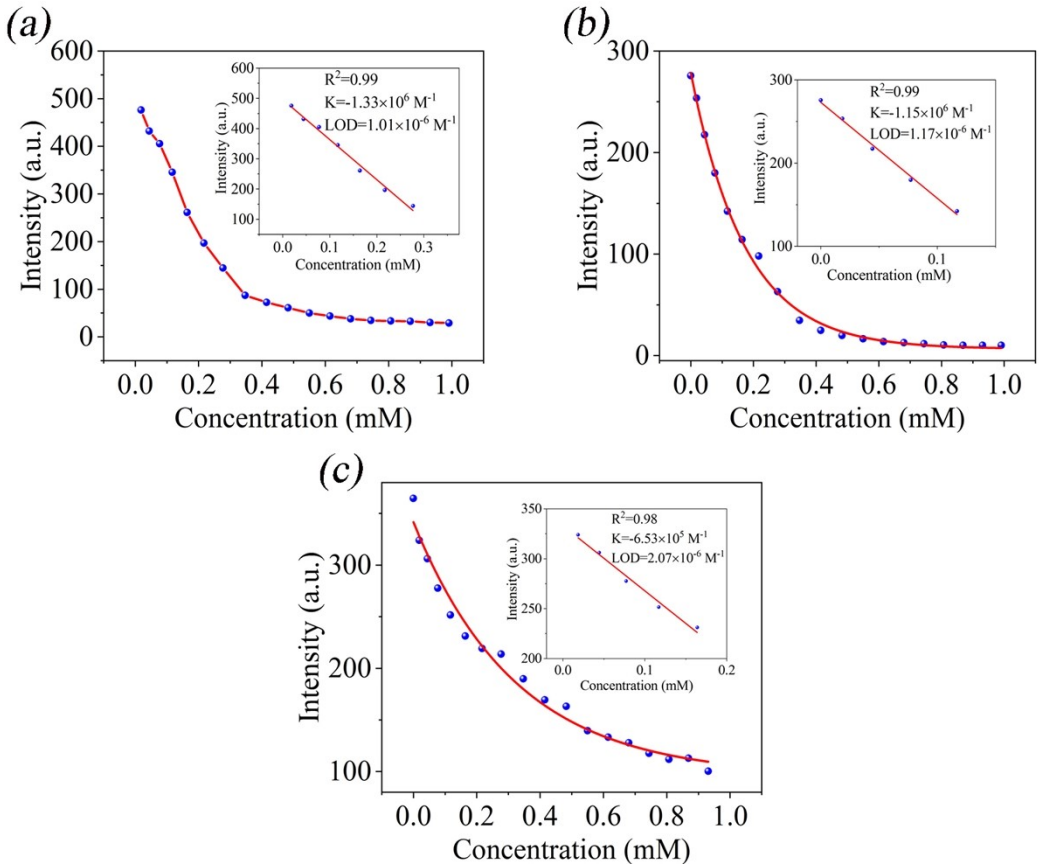

Figure S5 The plots of concentration vs. intensity and at low concentration with simulation equations of **MOFs 1-3**.

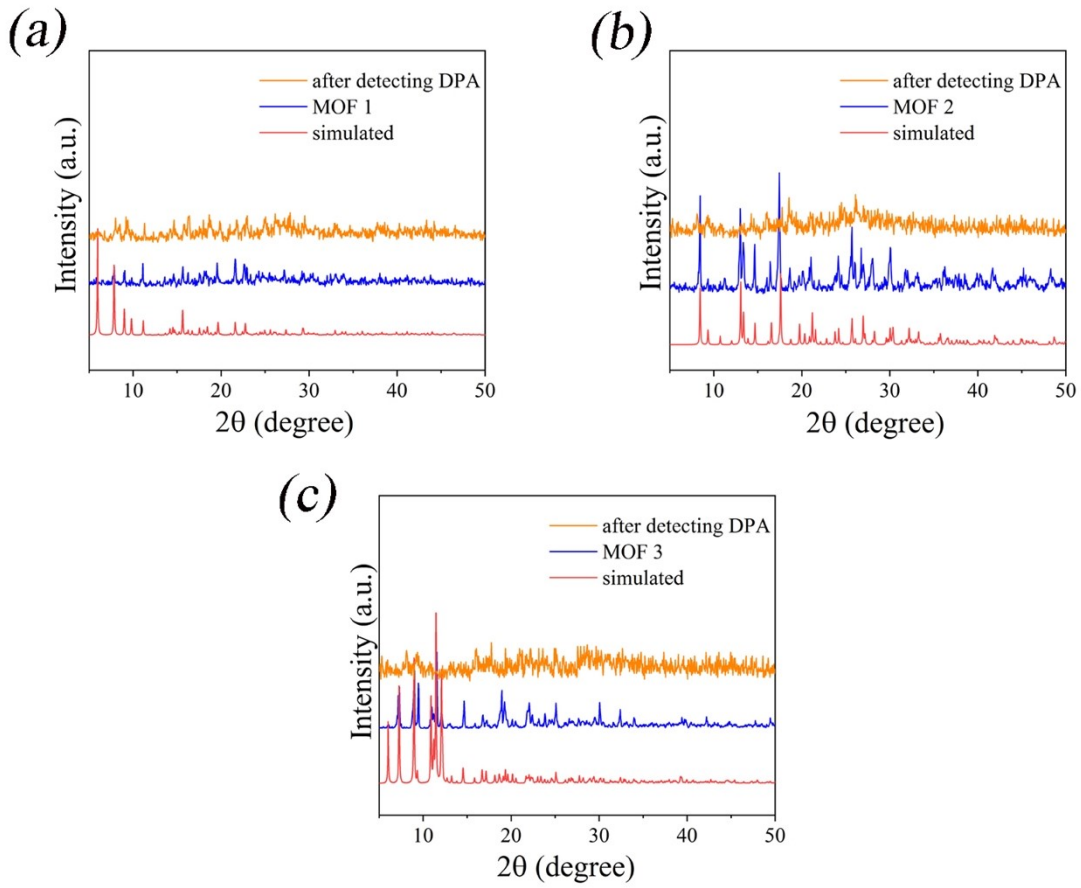

Figure S6 PXRD patterns of **MOFs 1-3** after detecting DPA.

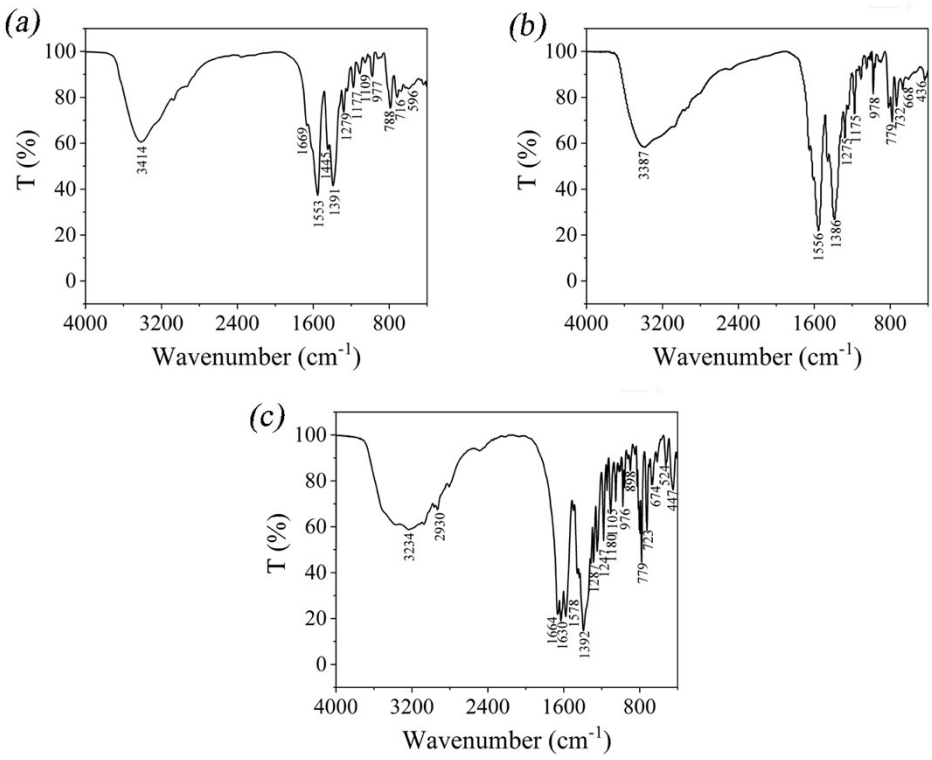

Figure S7 FT-IR spectra of **MOFs 1-3**.

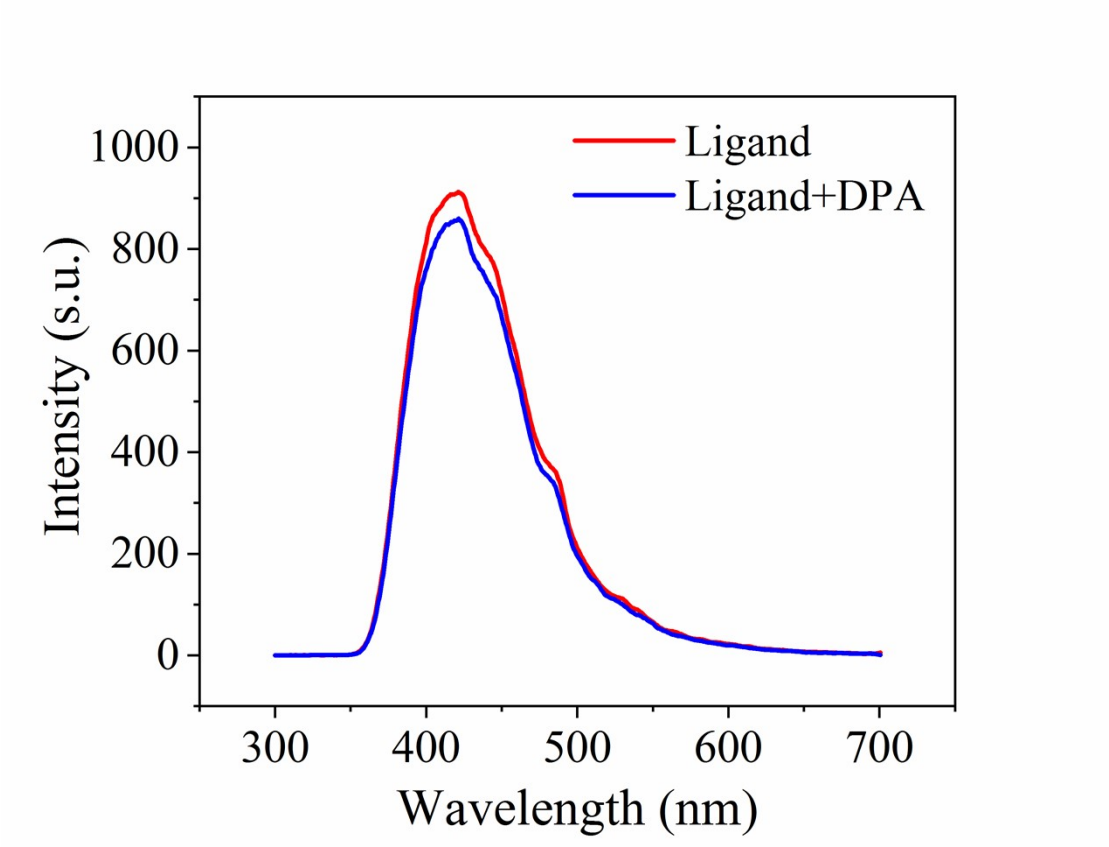

Figure S8 Fluorescence emission of ligand before and after PGA addition.

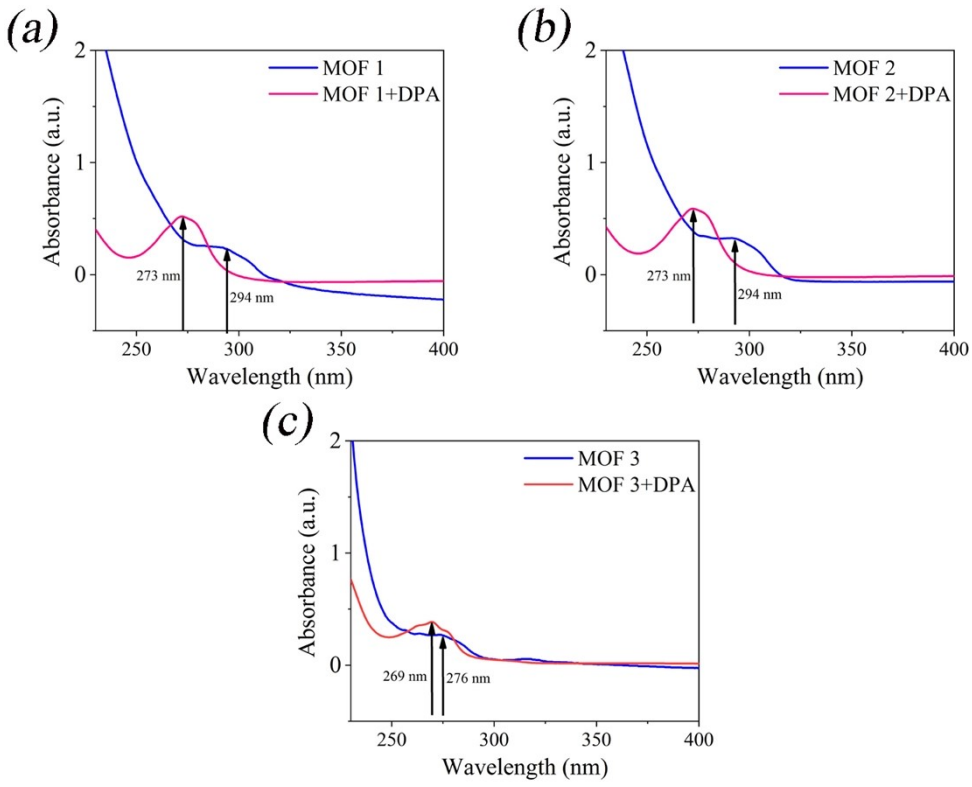

Figure S9 The comparison of UV spectra before and after addition of DPA.

Table S7 A comparison of limit of detection (LOD) of various methods for sensing DPA.

Methods	Sensor	LOD (μM)	Ref.
Fluorometric	**3**	0.248	S1
Fluorometric	**6**	0.874	S1
Fluorometric	**9**	2.277	S1
Colorimetric, fluorometric	EBT-Eu^{3+}	2	S2
Fluorometric	LP-Eu^{3+}	0.3	S3
Fluorometric	Pdots-Tb^{3+}	0.2	S4
Colorimetric, fluorometric	PV-Tb^{3+}	5	S5
Fluorometric	GNPs-Tb^{3+} and Eu^{3+}	1	S6
Colorimetric, fluorometric	BODIPY-Cu^{2+}	2	S7
Colorimetric	UCNPs-TPP/EBT	0.9	S8
fluorometric	**MOF 1**	1.01	This work
fluorometric	**MOF 2**	1.17	This work
fluorometric	**MOF 3**	2.07	This work

REFERENCE

S1 M.-L. Shen, B. Liu, L. Xu and H. Jiao, *Journal of Materials Chemistry C*, 2020, **8**, 4392-4400.

S2 M. D. Yilmaz and H. A. Oktem, Anal. Chem., 2018, 90, 4221.

S3 H. Seo, S. Singha and K. H. Ahn, Asian J. Org. Chem., 2017, 6, 1257.

S4 Q. Li, K. Sun, K. W Chang, J. B. Yu, D. T. Chiu, C. F. Wu and W. P. Qin, Anal. Chem., 2013, 85, 9087.

S5 K. J. Clear, S. Stroud and B. D. Smith, Analyst. 2013, 138, 7079.

S6 M. Donmez, M. D. Yilmaz and B. Kilbas, J. Hazard. Mater., 2017, 324, 593.

S7 Y. Cetinkaya, M. N. Z. Yurt, H. A. Oktem and M. D. Yilmaz, J. Hazard. Mater., 2019, 377, 299.

S8 Z. H. Chen, X. Liu, S. Q. Zhang, T. Yang, M. L. Chen and J. H. Wang, Anal. Chem., 2019, 91, 12094.